

## Inelastic Light Scattering from Magnetic Fluctuations in $\text{CuGeO}_3$

P. H. M. van Loosdrecht, J. P. Boucher, and G. Martinez

*Grenoble High Magnetic Field Laboratory, Max-Planck-Institut für Festkörperforschung and Centre National de la Recherche Scientifique, 25 Avenue des Martyrs, BP 166, F-38042 Grenoble Cedex 9, France*

G. Dhalenne and A. Revcolevschi

*Laboratoire de Chimie des Solides, Université de Paris-Sud, Bâtiment 414, F-91405 Orsay, France*

(Received 7 June 1995)

Magnetic fluctuations in  $\text{CuGeO}_3$  are studied using inelastic light scattering experiments over a broad temperature range. In the dimerized phase ( $T < 14$  K), scattering resulting from maxima in the magnonlike density of states and from spin-phonon coupled modes are reported. In the short-range order regime of the uniform phase ( $14 < T < 60$  K) the results confirm the existence of a spin-wave continuum, as expected for a one-dimensional quantum Heisenberg chain. At high temperatures ( $T > 60$  K) clear evidence is given for the existence of low-dimensional diffusive fluctuations.

PACS numbers: 75.40.Gb, 75.50.Ee, 78.30.Hv

The static and dynamic properties of low-dimensional systems show many unusual phenomena resulting from quantum effects and nonlinearity. In particular, an isotropic one-dimensional (1D) antiferromagnetic (AF) system has a gapless excitation spectrum for the case of half-integer spins, while it shows a gap in the case of integer spins [1]. However, due to the presence of small magnetoelastic couplings which always exist in real systems, a gap is also expected in the case of half-integer spins. This gap is the result of a dimerization of the lattice, directly induced by the magnetic fluctuations. Such a structural transition is the magnetic analog of the Peierls transition in metals, and, for that reason, has been dubbed the spin-Peierls transition. That remarkable phenomenon was first observed in organic materials and was widely investigated in the 1980s [2]. Recently such a dimerization effect was observed in the inorganic compound  $\text{CuGeO}_3$  [3]. In this compound, the spin-Peierls transition occurs at  $T_{\text{sp}} = 14$  K. Below  $T_{\text{sp}}$ , it is characterized by a rapid drop of the magnetic susceptibility  $\chi(T)$ , which is the signature of the opening of a gap in the magnetic excitation spectrum. In the dimerized (D) phase, i.e., for  $T < T_{\text{sp}}$ , this gap has been directly observed by neutron inelastic scattering (NIS) [4]. The associated dimerization of the lattice has been verified by x-ray and elastic neutron scattering [5,6]. Exchange interaction Raman scattering from spin fluctuations provides a suitable technique to study magnetic fluctuations in AF systems. This type of two-spin scattering is highly sensitive to structure in the density of states. For the spin-Peierls gap in  $\text{CuGeO}_3$ , this has recently been shown by Kuroe *et al.* [7].

The present Letter reports on polarized Raman scattering experiments performed in a wide temperature range, from 300 K down to a few kelvin. Pronounced features associated with magnetic fluctuations are observed not only in the D phase ( $T < T_{\text{sp}} = 14$  K), but also in the uniform (U) phase ( $T > T_{\text{sp}}$ ). In this U phase, a distinc-

tion is made between the short-range order (SRO) regime, for  $T_{\text{sp}} < T < T_{\text{max}}$  ( $\approx 60$  K) and the high-temperature (HT) regime for  $T > T_{\text{max}}$ , where  $T_{\text{max}}$  corresponds to the maximum observed in  $\chi(T)$  [3]. Strikingly different behaviors are observed in the spectra recorded in the three temperature ranges defined here. These observations are analyzed in terms of the magnetic fluctuation spectra expected for an antiferromagnetic quantum Heisenberg chain, i.e., a magnonlike dispersion in the D phase, spin-wave continuum fluctuations in the SRO regime, and a diffusive behavior at high temperatures.

$\text{CuGeO}_3$  has an orthorhombic structure with space group  $Pbmm$  [8]. The magnetic chains are formed by the  $S = 1/2$   $\text{Cu}^{2+}$  ions running along the  $c$  axis of the crystal. The magnetic interaction is described by the isotropic Heisenberg Hamiltonian  $H = \sum_i 2J_i \mathbf{S}_i \cdot \mathbf{S}_{i+1}$ , with an intrachain exchange coupling  $J = J_c \approx 60$  K, and in the D phase a small interchain interaction in the  $b$  direction  $J_b \approx 0.1J_c$  (the coupling along the  $a$  axis is much smaller and will be neglected hereafter) [4]. Samples used in this study were grown from the melt by a floating zone technique [9]. Cleaved perpendicular to the (100) direction, they show a very good optical quality. Samples were mounted in a cold finger flow cryostat providing a temperature accuracy of about 1 K. Raman spectra have been recorded in a backscattering geometry using a charge coupled device equipped spectrometer (Dilor XY). The 514 nm line of an Ar-ion laser was used for excitation, keeping the intensity below  $200 \text{ W/cm}^2$  to minimize local heating. Experiments have been performed in a  $(\mu\nu)$  scattering geometry, where  $\mu, \nu$  denote the polarization of the incident and scattered light, respectively. Magnetic scattering is observed only in the  $(zz)$  geometry, with  $z \parallel c$ . Examples of the experimental observations are given in Fig. 1. In the D phase [Fig. 1(a)], four distinct peaks are clearly seen, in addition to the phonon peaks at 184 and  $330 \text{ cm}^{-1}$ . In the SRO regime

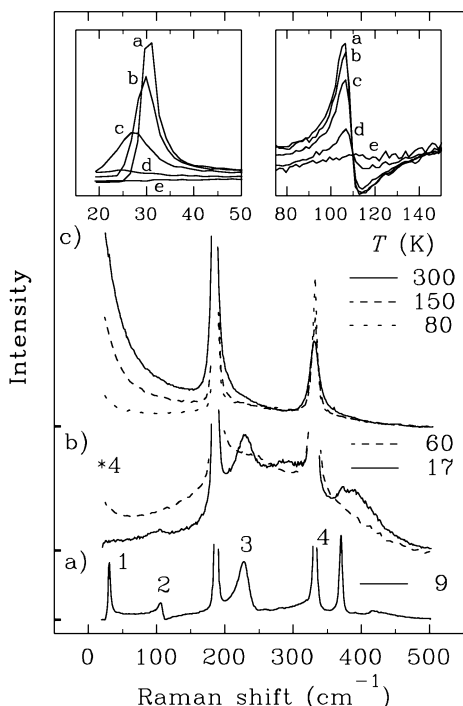


FIG. 1. Raman spectra of  $\text{CuGeO}_3$  recorded in  $(zz)$  geometry at (a)  $T = 9$  K, (b)  $T = 17$  and  $60$  K (scaled up by a factor 4), and (c)  $T = 80, 150,$  and  $300$  K. The insets show a detailed temperature dependence [ $T =$  (a)  $9$ , (b)  $11$ , (c)  $13$ , (d)  $15$ , (e)  $17$  K] of the features observed at low temperatures around  $32$  and  $106$   $\text{cm}^{-1}$ .

[Fig. 1(b)], the magnetic fluctuations give rise to broad maxima at relatively high energy ( $\sim 230$   $\text{cm}^{-1}$ ), while in the HT regime [Fig. 1(c)] these fluctuations are observed to be transferred toward low energy to form a quasi-diverging central peak.

For the exchange scattering process, the matrix element  $M$  for the interaction of light with the magnetic system is of the form  $M = \sum_i \sum_s A_s \mathbf{S}_i \cdot \mathbf{S}_{i+s}$ , where  $i$  labels the spins and  $s$  their nearest neighbors.  $A_s$  depends on the magnitude and polarization of the light, and on the symmetry of the magnetic fluctuations [10]. For crossed polarization of the incoming and scattered light,  $A_s$  vanishes by symmetry in  $\text{CuGeO}_3$ . For parallel polarization,  $A_s$  is proportional to the squared exchange interaction between nearest neighbors along the polarization direction. One thus expects the strongest contribution to inelastic light scattering in  $(zz)$  geometry, as is the case experimentally. Accordingly, the Raman scattering intensity can be written as

$$I(\omega) \propto \sum_{\mathbf{q}} f_{\mathbf{q}} \langle S_{\mathbf{q}}^{\alpha}(t) S_{-\mathbf{q}}^{\alpha}(t) S_{\mathbf{q}}^{\alpha}(0) S_{-\mathbf{q}}^{\alpha}(0) \rangle_{\omega}, \quad (1)$$

where  $\alpha = x, y, z$ , and  $\mathbf{q} = (q, k)$  are the wave vectors associated with the two-dimensional reciprocal space spanned by the  $c^*$  and  $b^*$  axes of the crystal, respectively.

In the following, the wave vectors are defined within the AF Brillouin zone, and the interatomic distances are taken to be unity ( $a = b = 1$ ). In Eq. (1),  $f_{\mathbf{q}} = \cos^2(q/2)$  appears as a “filtering” function which emphasizes the contributions of fluctuations in the first half of the Brillouin zone.

Consider first the results obtained in the D phase [Fig. 1(a)]. Several well-defined features are observed which disappear above  $T_{\text{sp}}$ . First, a narrow peak (peak 1) is observed around  $32$   $\text{cm}^{-1}$ , with a sharp cutoff at the lower energy side and a tail towards higher energy. Second, a strongly asymmetric peak (peak 2) is observed around  $106$   $\text{cm}^{-1}$ . Third, a broad continuum is observed, peaking near  $230$   $\text{cm}^{-1}$  (peak 3), with a relatively sharp cutoff on the high energy side. Fourth, a relatively strong almost-Lorentzian-shaped peak (peak 4) is observed near  $369$   $\text{cm}^{-1}$ .

The analysis of this rich spectrum is made in two steps, the first step considering only purely magnetic contributions. The magnetic excitation spectrum in the D phase of  $\text{CuGeO}_3$  is relatively well known from NIS experiments [4,11]. It is characterized by well-defined propagative modes with marked dispersions  $\omega_{\mathbf{q}}$ . A sketch of the dispersion curves is given in the left inset of Fig. 2. Because of the interchain coupling  $J_b$ , two different gaps occur due to the dimerization of the lattice, at different points of the reciprocal space [12]. The lowest gap ( $E_{g1} = 16$   $\text{cm}^{-1}$ ) is found at  $(q, k) = (\pi, \pi)$  and  $(0, \pi)$ , while the highest one ( $E_{g2} = 45$   $\text{cm}^{-1}$ ) is located at  $(q, k) = (0, 0)$  and  $(0, \pi)$ . Although the magnetic modes are not purely elementary excitations (they are certainly better described in terms of continua of elementary excitations [2]), one may apply here the description given for magnon modes. This allows one to rewrite Eq. (1) as  $I(\omega) \propto \sum_{\mathbf{q}} f_{\mathbf{q}} \delta(\omega - 2\omega_{\mathbf{q}})$ . In the D phase, the Raman scattering intensity then results from processes involving two magnonlike excitations of equal energy and opposite wave vector. Replacing the delta functions by Lorentzians to describe the magnonlike modes at  $\omega_{\mathbf{q}}$  one numerically obtains spectrum (a) shown in Fig. 2. In this evaluation, the limited short-range order—of the order of 3 and 1 lattice units along the  $c$  and  $b$  directions, respectively [4,11]—have been taken into account. The only adjustable parameters are the energy widths of each Lorentzian. They are of the order of  $0.7$   $\text{cm}^{-1}$  for modes with  $q \sim 0$ , and of the order of  $2$   $\text{cm}^{-1}$  for those with  $q \sim \pi/2$ . Clearly, the simulated spectrum reproduces peaks 1 and 3 fairly well. The peaks in the model calculation correspond to maxima in the magnonlike density of states. Using this simple model, one can now assign peak 1 to the gap at  $(q, k) = (0, \pi)$ , and peak 3 to the maximum of the dispersion curves observed at  $q = \pi/2$ . One could also assign peak 2 to the gap at  $(q, k) = (0, 0)$ . The temperature dependence of this peak, however, does not correspond to what one expects for a spin-Peierls gap. Approaching  $T_{\text{sp}}$  from

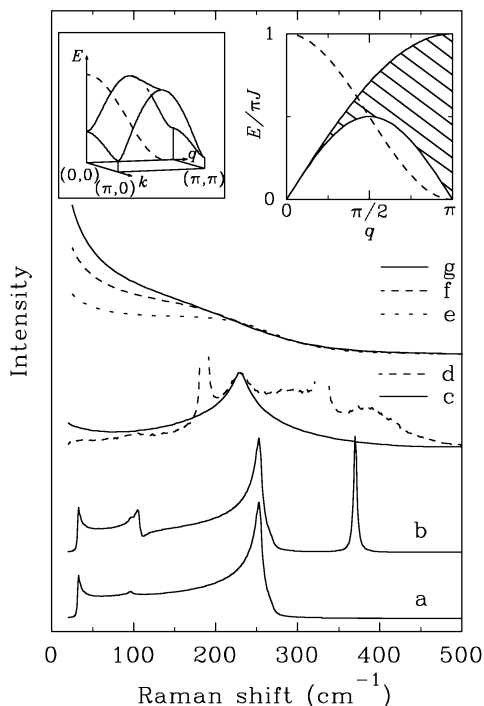


FIG. 2. Model simulations of the scattered Raman intensity in (a), (b) the D phase, and in (c) the SRO and (e) HT [(e) 80 K, (f) 150 K, and (g) 300 K] regimes of the U phase in  $\text{CuGeO}_3$ , as discussed in the text. For comparison the experimental spectrum for  $T = 17$  K [Fig. 1(b)] is replotted here [curve (d)]. Insets: Sketch of the dispersion of magnonlike excitations in the D phase (left) and continuum of states in the SRO regime of the U phase (right). The dashed curves in the insets show the filtering function defined in the text.

below, this peak should broaden and shift to zero, as is observed for peak 1. This is not the case (compare the insets in Fig. 1), however, and an alternative interpretation is given below. Similarly, it is clear that peak 4 cannot be explained in this purely magnetic model.

The second step of the analysis therefore considers the possibility of vibrational scattering together with spin-phonon coupling. Peak 2 may result from a zone boundary phonon, whose activity is induced in the D phase by the zone folding due to the dimerization, while the typical asymmetry strongly suggests a Fano type of coupling [13] to the magnonlike continuum of states. In a simple approximation the line shape for such a coupled spin-phonon process can be expressed as  $I(\omega) = I_c(\lambda + \epsilon)^2/(1 + \epsilon^2)$ , where  $I_c$  is the scattered intensity of the uncoupled continuum,  $\lambda$  is the Fano parameter denoting the spin-phonon coupling, and  $\epsilon = (\omega - \omega_0)/\gamma$ , with  $\omega_0$  the unperturbed phonon frequency and  $\gamma$  the linewidth parameter. A satisfactory fit of this equation to the data of Fig. 1(a) yields  $\omega_0 = 107 \text{ cm}^{-1}$ ,  $\lambda = -1.5$ , and  $\gamma = 3 \text{ cm}^{-1}$ . Recent NIS investigations indeed found several modes at the  $c^*$  zone boundary around  $107 \text{ cm}^{-1}$  [14]. Figure 2(b) shows a simulation which includes such a Fano mode with the experimentally determined param-

eters. In this simulation, the phonon around  $107 \text{ cm}^{-1}$  has been coupled only to part of the continuum (30%) to account for the fact that the calculated magnetic contributions in this energy range overestimate the observed intensity.

As peak 2, peak 4 may also be attributed to a zone boundary phonon which is activated due to the dimerization. Including a simple Lorentzian to account for this mode, the simulated spectrum of Fig. 2(b) shows a good overall agreement with the experimental result.

Now consider the results obtained in the uniform phase. Obviously, the features described above have completely disappeared. In the SRO regime [Fig. 1(b)], only a broad continuum is observed, which extends from (nearly) zero up to about  $450 \text{ cm}^{-1}$  [Fig. 1(c)]. These spectra can be understood in terms of the description usually given for  $S = 1/2$  Heisenberg chains [15]. For such a quantum spin system, important fluctuations are present even at  $T = 0$ . They are expected to form a continuum of elementary excitations between the limits  $E_1 = \pi J |\sin(q)|$  and  $E_2 = 2\pi J |\sin(q/2)|$ . Such a spin-wave continuum—the intensity of which is characterized by a square root divergence at its lowest limit—is represented by the hatched area in the inset of Fig. 2 (right). The most intense and extended modes are located around  $q = \pi$ . However, due to the filtering function (shown as the dashed line in the same inset), these modes are not observed in Raman scattering. At  $T > 0$ , one expects these magnetic modes to be damped by thermal fluctuations. Introducing such a damping (through a single parameter  $\gamma = 3 \text{ cm}^{-1}$ ) in the above description, and assuming two-mode processes as has been done before for the D phase, their contribution to the Raman scattering intensity is calculated using Eq. (1). The resulting spectrum [Fig. 2(c)] shows a broad maximum around  $230 \text{ cm}^{-1}$ , in good agreement with the experimental spectrum for  $T = 17$  K, which for comparison is replotted in the same figure [curve (d)]. The position of the peak, which is due to modes around  $q = \pi/2$ , gives, through  $E_1$ , a direct estimate of the exchange coupling. The value deduced here,  $J_c = 60$  K, is found to be in good agreement with the determination from  $\chi(T)$  measurements [3]. The additional scattering observed at the high energy side of the maximum is due to higher order processes involving two spin excitations and a phonon, as is strongly indicated by recent pressure dependent experiments [16].

The strongest fluctuations are definitely observed in the HT regime, i.e., for  $T > T_{\text{max}}$ . In Fig. 1(c) they are seen to develop at low energy, and to increase with  $T$  increasing. These fluctuations can be understood in terms of a diffusive behavior, which, in low-dimensional systems, is known to yield a divergence in the energy spectrum as  $E \rightarrow 0$  [17]. In the experiments, the diffusion is that of the four-spin correlation functions involved in Eq. (1). For such functions, the conserved quantity which justifies a

diffusive behavior is constructed from the operator  $\mathcal{N} = \sum_i S_i^\alpha S_{i+n}^\alpha$ , which, after summation over  $n$ , can be checked to commute with the isotropic Heisenberg Hamiltonian [18]. In the infinite  $T$  limit, several important results have been established: The diffusion coefficient  $D_4$  is about twice the corresponding coefficient  $D_2$  of the two-spin correlation functions, and the quantity  $D_2/JS(S+1)$  depends little on the spin value [19]. Accordingly, one can use, as a first approach, the results known for classical spins. The experiments do not really probe the purely diffusive regime for  $E \rightarrow 0$ . Rather, they cover a region higher in energy than the purely diffusive regime, which can be described by the “memory function approach”—in its simplest Gaussian limit—proposed first by Tahir-Kheli and McFadden [20]. This approach allows one to construct any individual magnetic  $q$  modes in terms of their frequency moments, the  $T$  dependence of which is known for classical spin chains only [21]. Using the above formalism curves, Figs. 2(e), 2(f), and 2(g), we obtain  $T = 80, 150, 300$  K, respectively. This simple model qualitatively reproduces the experimentally observed increase of intensity towards lower energy and the temperature dependence. This behavior is a result of a transfer of intensity from the AF fluctuations at  $q \sim \pi$  to diffusive modes at  $q \sim 0$  as  $T$  increases.

To summarize, in the D phase the magnetic fluctuations are found to be magnonlike, in agreement with previous NIS experiments. Additionally, it is shown that strong spin-phonon couplings exist in the D phase. This result is of particular interest in view of the magnetoelastic spin-Peierls transition in this compound. In the SRO regime of the U phase the existence of a spin-wave continuum, characteristic for a uniform Heisenberg system, is evidenced by the broad structure observed in the spectra which peaks around  $230 \text{ cm}^{-1}$ . The quasidiverging central peak observed in the HT regime of the U phase clearly demonstrates a low-dimensional diffusive behavior of the spin fluctuations.

The authors wish to thank L.P. Regnault and M. Aïn for valuable discussions. The Grenoble High Magnetic

Field Laboratory is “Laboratoire associé à l’Université Joseph Fourier de Grenoble.” Partial financial support by the New Energy Development Organization is gratefully acknowledged.

- 
- [1] F.D.M. Haldane, Phys. Rev. Lett. **50**, 1153 (1983).
  - [2] J.W. Bray *et al.*, in *Extended Linear Chain Compounds*, edited by J.S. Miller (Plenum Press, New York, 1983), Vol. 3.
  - [3] M. Hase, I. Terasaki, and K. Uchinokura, Phys. Rev. Lett. **70**, 3651 (1993).
  - [4] M. Nishi, O. Fujita, and J. Akimitsu, Phys. Rev. B **50**, 6508 (1994).
  - [5] J.P. Pouget *et al.*, Phys. Rev. Lett. **72**, 4037 (1994).
  - [6] K. Hirota *et al.*, Phys. Rev. Lett. **73**, 736 (1994).
  - [7] H. Kuroe *et al.*, Phys. Rev. B **50**, 16468 (1994).
  - [8] H. Völlenkle, A. Wittman, and N. Nowotny, Monatsh. Chem. **98**, 1352 (1967).
  - [9] A. Revcolevschi and R. Collongues, C.R. Acad. Sci. **266**, 1767 (1969).
  - [10] P.A. Fleury and R. Loudon, Phys. Rev. **166**, 514 (1968).
  - [11] L.P. Regnault *et al.*, Physica (Amsterdam) (to be published).
  - [12] T.M. Brill *et al.*, Phys. Rev. Lett. **73**, 1545 (1994).
  - [13] U. Fano, Phys. Rev. **124**, 1866 (1961).
  - [14] M. Aïn (private communication).
  - [15] G. Müller, H. Thomas, H. Beck, and J.C. Bonner, Phys. Rev. B **24**, 1429 (1981).
  - [16] P.H.M. van Loosdrecht *et al.* (unpublished).
  - [17] H. Benner and J.P. Boucher, in *Magnetic Properties of Layered Transition Metal Compounds*, edited by L. de Jongh (Kluwer Academic Press, Dordrecht, 1989).
  - [18] Y. Barjhoux, J.P. Boucher, and J. Cibert, J. Appl. Phys. **50**, 1764 (1979).
  - [19] F. Ferrieu, J. Phys. (Paris) **38**, L381 (1977).
  - [20] R.A. Tahir-Kheli and D.G. McFadden, Phys. Rev. **182**, 604 (1969).
  - [21] H. Tomita and H. Mashiyama, Prog. Theor. Phys. **48**, 1133 (1972).